

Supplementary Materials

Electrochemical degradation of ciprofloxacin with a Sb-doped SnO₂ electrode: Performances, influencing factors and degradation pathways

Yanguang Mu^a, Cong Huang^a, Haipu Li ^{a,b*}, Leilei Chen^a, Ding Zhang^a, Zhaoguang

Yang ^{a,b*}

^a Center for Environment and Water Resources, College of Chemistry and Chemical

Engineering, Central South University, Changsha 410083, PR China

^b Key Laboratory of Hunan Province for Water Environment and Agriculture Product

Safety, Changsha 410083, PR China

*Corresponding author.

E-mail addresses: lihaipu@csu.edu.cn (Haipu Li), zgyang@csu.edu.cn (Zhaoguang

Yang)

Captions

Text S1 Analysis of intermediates with the Liquid Chromatography-mass spectrometry

Table S1 Crystallite size, lattice parameters, A, and C_{dl} of different electrodes.

Table S2 Comparison of EIS results as determined by the equivalent circuit fit.

Table S3 Summary of removal rates and kinetic constants of CIP (90 min).

Table S4 The possible intermediate products in the CIP degradation

Fig. S1 CV curves of electrodes in 0.1 M KCl solution containing 1 mM K₃Fe(CN)₆:

(a) SSO-8, (b) SSO-10, (c) SSO-12, (d) SSO-14, (e) SSO-16, and (f) SSO-20.

23 **Fig. S2** CV curves of different electrodes in 0.5 M KOH solution: (a) SSO-8, (b)
24 SSO-10, (c) SSO-12, (d) SSO-14, (e) SSO-16, and (f) SSO-20.

25 **Fig. S3** Three-dimensional excitation-emission matrix fluorescence spectra of the CIP
26 solution after electrocatalytic degradation of 0 min, 15 min, 30 min, 45min, 60min,
27 and 90 min under the optimal conditions.

28 **Fig. S4** CV curves of the SSO-16 electrode with the absence and presence of CIP.

29 **Fig. S5** Fluorescence spectral of electrochemical oxidation of 0.5 mM terephthalic
30 acid solution with the SSO-16 electrode.

31 **Fig. S6** TOC removal ratio as a function of time under the optimal degradation
32 conditions.

33 **Fig. S7** Relative intensity variations of intermediates during the process of CIP
34 degradation.

35 **Fig. S8** SEM image of the SSO-16 electrode after eight cycles of experiment.

36 **Fig. S9** The XRD pattern of the SSO-16 electrode after eight cycles of experiment.

37 Text S1 Analysis of intermediates with the Liquid Chromatography-mass
38 spectrometry

39 The degradation intermediates were analyzed by an Agilent 6460 triple quadrupole
40 mass spectrometer equipped with an electrospray ionization (ESI) source, combined
41 with an Agilent 1260 series Liquid Chromatography system. Chromatographic
42 separation was carried out with an Agilent Zorbax Bonus-RP column (2.1 mm i.d. ×
43 50 mm, particle size 2.7 μm). The mobile phase consisted of A (water with 0.1%
44 formic acid as a modifier) and B (methanol). The mobile-phase gradient was as
45 follows: 0 min, B 20%; 7 min, B 60%; 15 min, B 80%, and then returned to the initial
46 conditions within 1 min. The total run time was 22 min. The analytes were determined
47 in positive ionization mode, using the following MS operation parameters: capillary
48 voltage: 4000 V (+); nebulizer pressure: 40 psi; drying gas: 8 L min⁻¹; source
49 temperature: 350°C. The collision energy was selected according to the requirements
50 of the different measurements.

51

52 **Table S1** Crystallite size, lattice parameters, A , and C_{dl} of different electrodes

Electrode	Crystallite size (nm)	Lattice parameters		A^b (cm ²)	C_{dl}^c (mF)
		a = b (Å)	c (Å)		
SSO-8	246.1	4.754	3.113	2.35	1.65
SSO-10	45.6	4.749	3.193	2.16	1.49
SSO-12	14.8	4.710	3.164	3.4	7.07
SSO-14	12.2	4.709	3.196	3.53	2.72
SSO-16	28.6	4.673	3.198	3.74	5.83
SSO-20	37.2	4.720	3.143	2.88	0.45
Standard ^a	-	4.738	3.187	-	-

53 ^a The lattice parameters of SnO₂ (JCPDF 72-1147).

54 ^b Electrochemical active area.

55 ^c Electrochemical double layer capacitance.

56 **Table S2** Comparison of EIS results as determined by the equivalent circuit fit.

Electrode	R_e ($\Omega \text{ cm}^2$)	Q_{dl} ($\times 10^{-5}$)	n	R_{ct} ($\Omega \text{ cm}^2$)	C_{ads} ($\mu\text{F cm}^{-2}$)	R_{ads} ($\Omega \text{ cm}^2$)
SSO-8	8.30	7.91	0.79	865.70	47.43	234.5
SSO-10	6.93	19.20	0.86	17.05	53.40	123.8
SSO-12	7.80	60.36	0.86	5.97	270.30	115.9
SSO-14	6.06	67.93	0.90	8.85	210.91	68.4
SSO-16	7.08	49.38	0.82	8.46	222.32	186.2
SSO-20	7.71	8.40	0.90	49.94	0.079	291.5

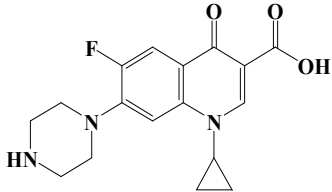
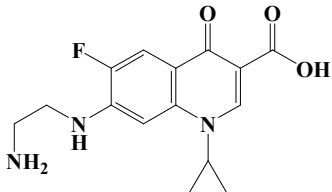
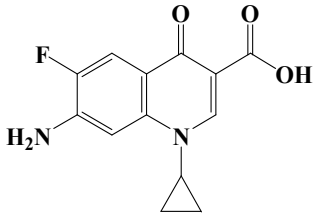
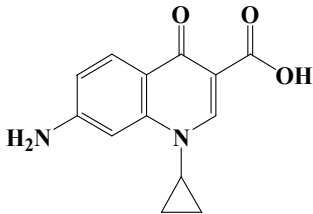
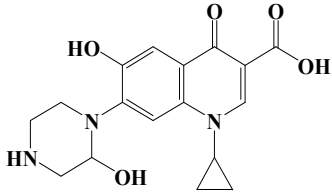
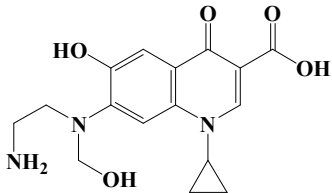
Table S3 Summary of removal rate and kinetic constants of CIP (90 min)

		Removal rate /%	k /min ⁻¹	R ²
Electrode ^a	SSO-8	60.99	0.0110	0.987
	SSO-10	66.06	0.0125	0.991
	SSO-12	91.63	0.0282	0.995
	SSO-14	89.43	0.0262	0.988
	SSO-16	96.24	0.0355	0.995
	SSO-20	79.47	0.0174	0.988
Current density (mA cm⁻²) ^b	10	86.65	0.0232	0.983
	15	96.24	0.0355	0.995
	20	97.78	0.0429	0.994
	25	99.77	0.0682	0.988
Electrolyte concentration (g L⁻¹) ^c	10	82.61	0.0203	0.989
	20	97.78	0.0429	0.994
	25	99.18	0.0506	0.982
	30	92.14	0.0292	0.988
	40	89.90	0.0266	0.991
Initial concentration (mg L⁻¹) ^d	10	99.90	0.0918	0.986
	30	99.18	0.0506	0.978
	50	92.21	0.0297	0.987
	80	74.01	0.0154	0.989
pH value ^e	3	99.97	0.0733	0.990
	5	99.18	0.0506	0.978
	7	99.44	0.0571	0.994
	9	99.30	0.0547	0.992

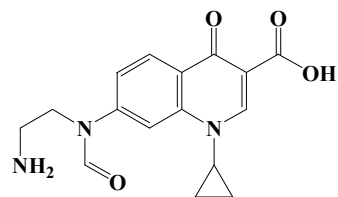
59 The operating conditions of each group of experiments: ^a Current density = 15 mA cm⁻², Na₂SO₄
60 concentration = 25 g L⁻¹, initial CIP concentration = 30 mg L⁻¹, and initial pH = 5; ^b Na₂SO₄
61 concentration = 25 g L⁻¹, initial CIP concentration = 30 mg L⁻¹, and initial pH = 5; ^c Current

62 density = 20 mA cm⁻², initial CIP concentration = 30 mg L⁻¹, and initial pH = 5. ^d Current density
63 = 20 mA cm⁻², Na₂SO₄ concentration = 25 g L⁻¹, and initial pH = 5. ^e Current density = 20 mA
64 cm⁻², Na₂SO₄ concentration = 25 g L⁻¹, and initial CIP concentration = 30 mg L⁻¹.
65

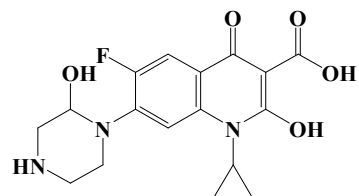
66 **Table S4** The possible intermediate products in the process of CIP degradation

Intermediates	[M+H] ⁺ m/z	Feature fragment m/z (relative intensity)	Structural formula
CIP	332	314 (100), 231 (85)	
A	306	288 (100), 165 (36)	
B	263	245(100), 204(34)	
C	245	204 (100), 41 (57)	
D	346	330 (100), 302 (30)	
E	334	316 (100), 216 (68), 72 (47)	

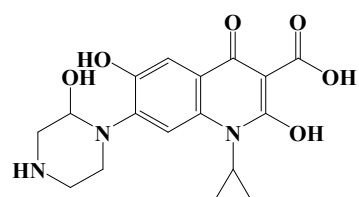
F 316 217 (100), 72 (50), 230 (23)



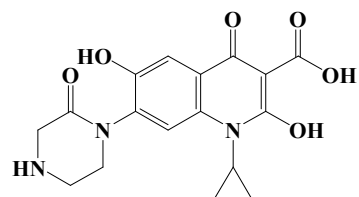
G 364 346(100), 330 (77)



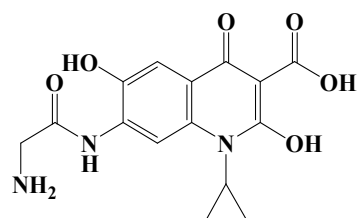
H 362 344(100)



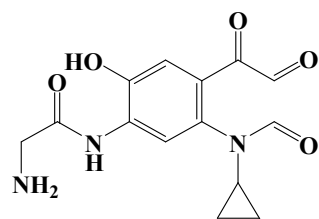
I 360 344(100)

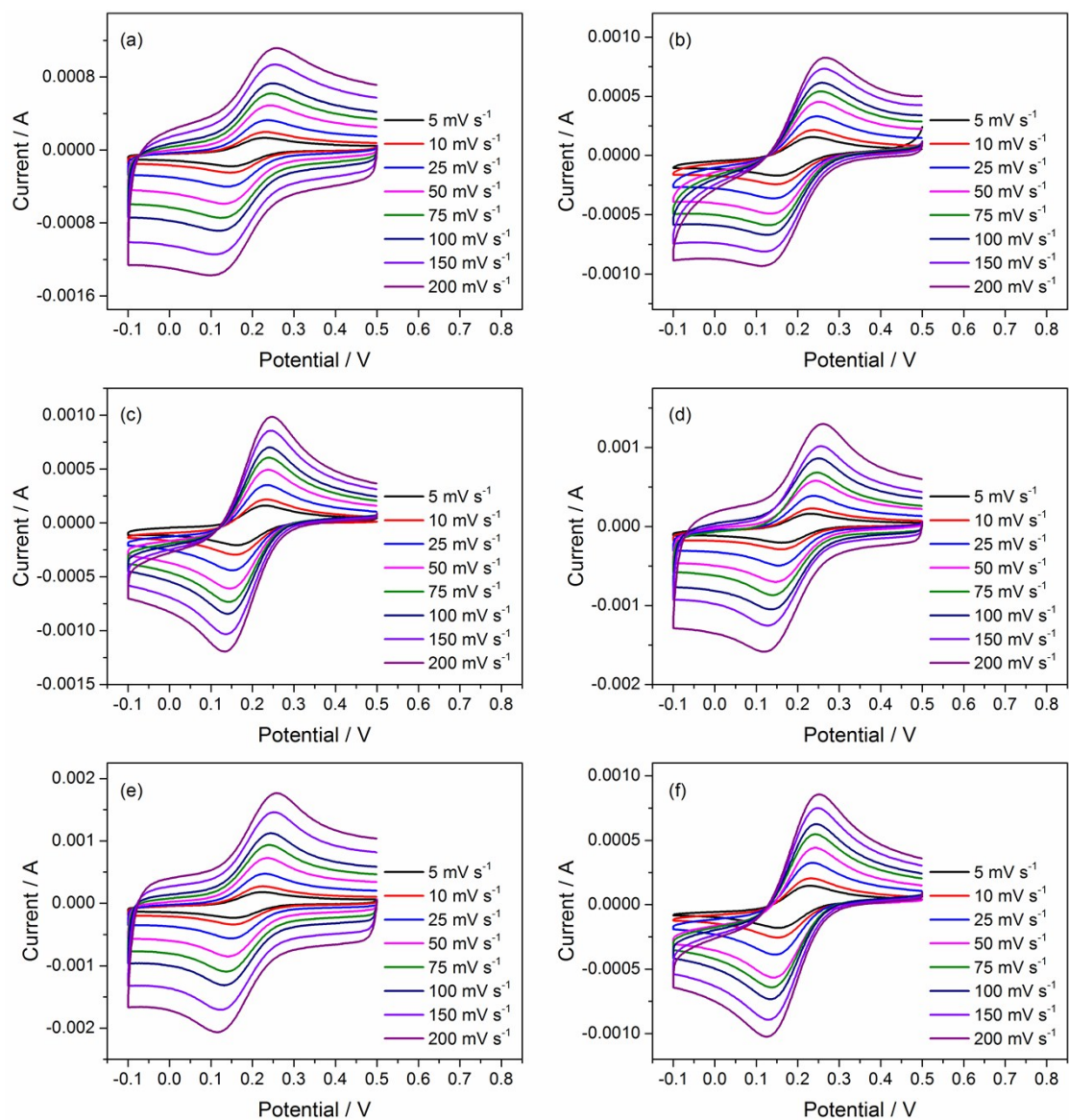


J 334 316 (100), 229 (32), 245 (16)



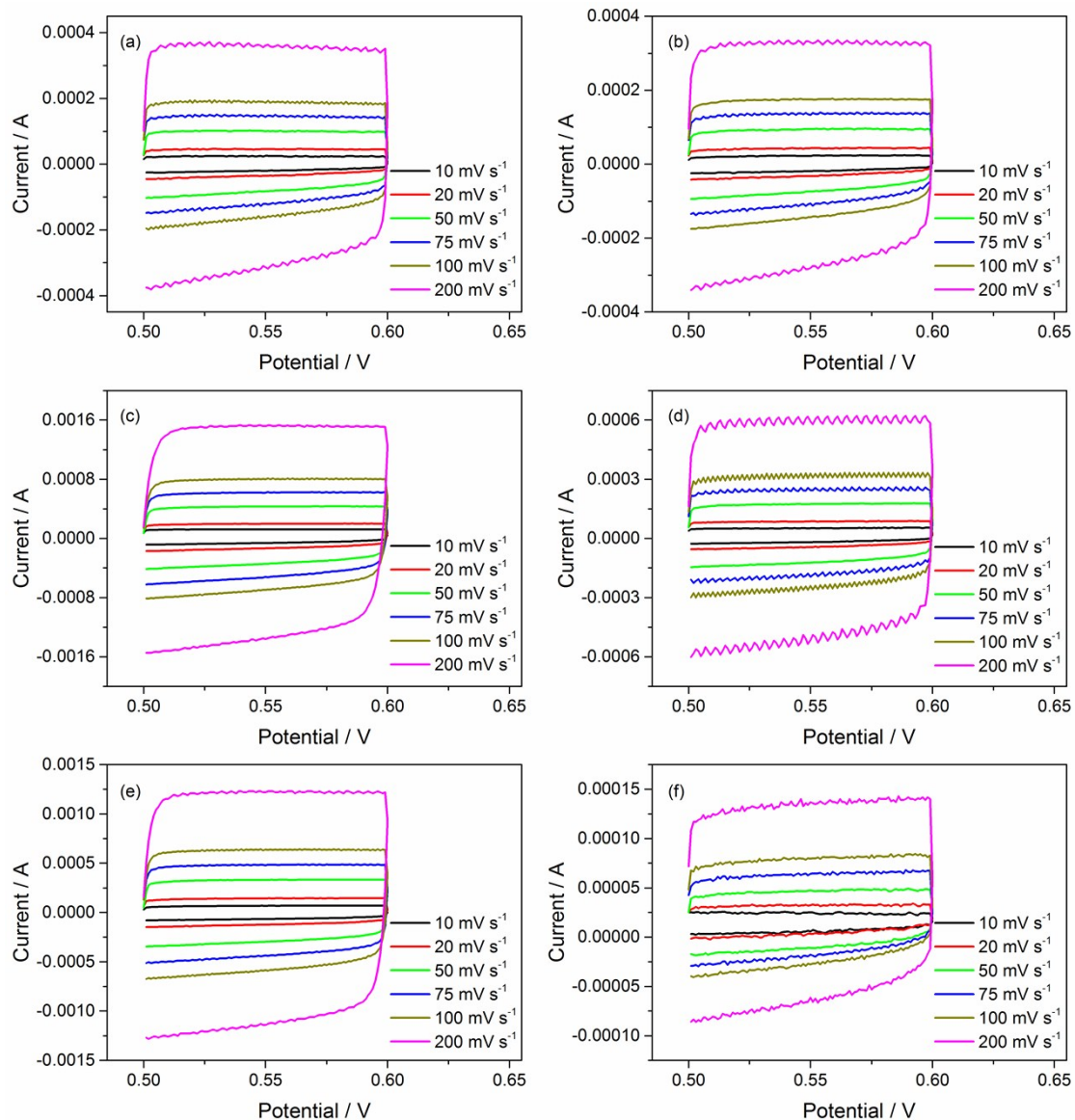
K 306 227 (100), 217 (95), 190 (53)





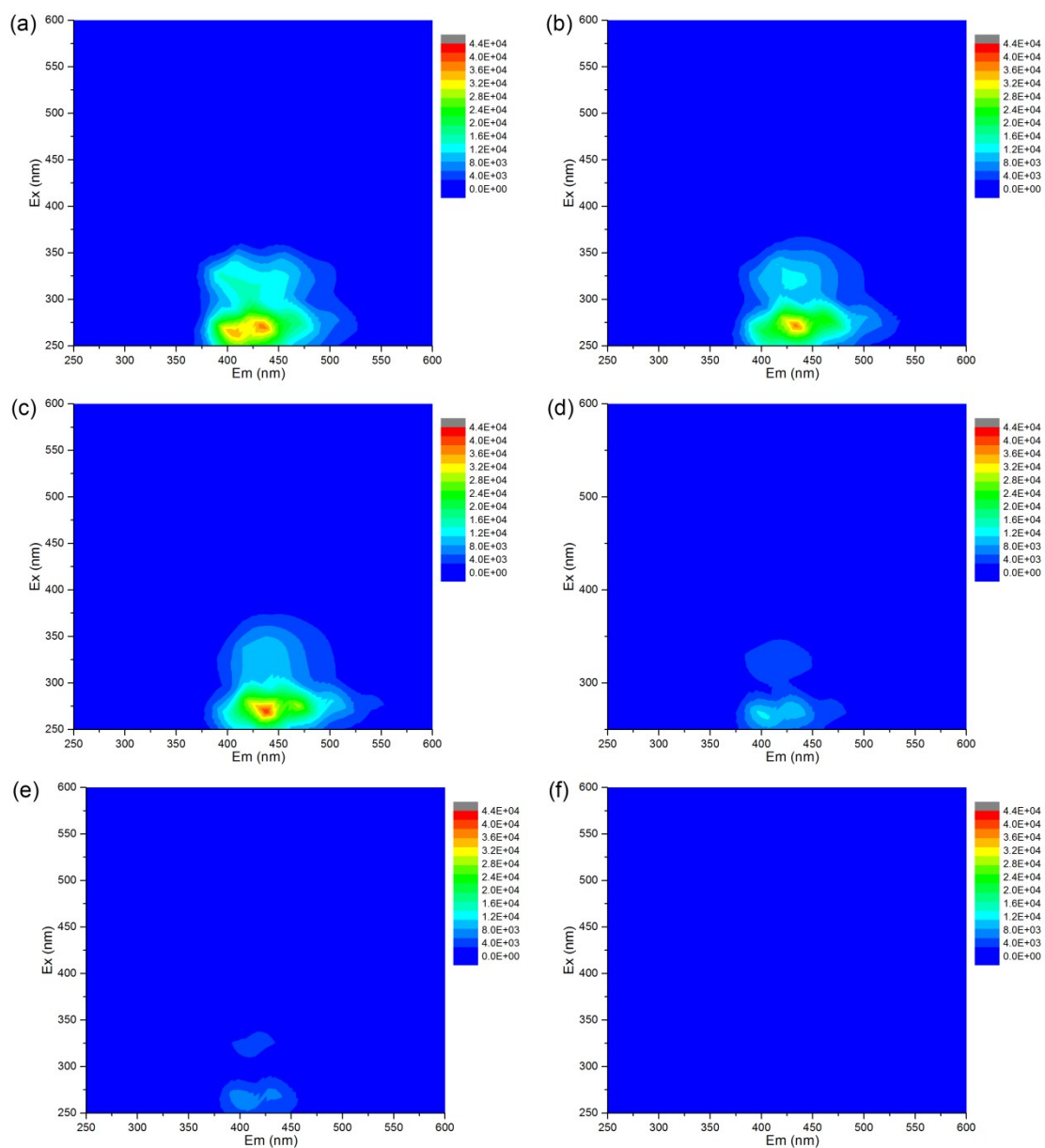
68

69 **Fig. S1** CV curves of electrodes in 0.1 M KCl solution containing 1 mM $K_3Fe(CN)_6$, (a) SSO-8, (b)
 70 SSO-10, (c) SSO-12, (d) SSO-14, (e) SSO-16, and (f) SSO-20.



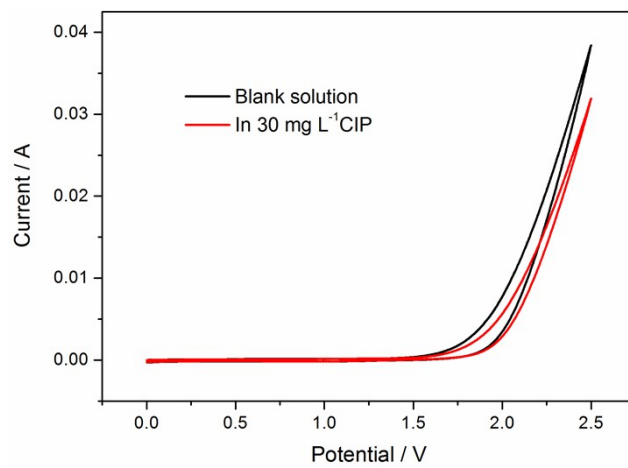
71
72
73

Fig. S2 CV curves of different electrodes in 0.5 M KOH solution: (a) SSO-8, (b) SSO-10, (c) SSO-12, (d) SSO-14, (e) SSO-16, and (f) SSO-20.



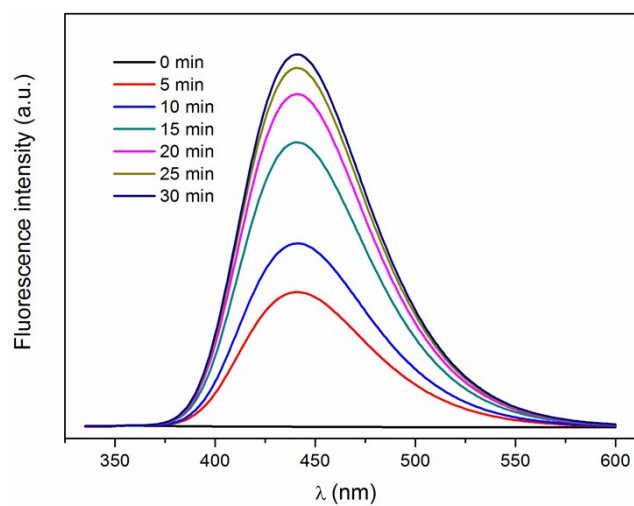
74

75 **Fig. S3** Three-dimensional excitation-emission matrix fluorescence spectra of the CIP solution
 76 after electrocatalytic degradation of 0 min, 15 min, 30 min, 45min, 60min, and 90 min under the
 77 optimized conditions (Current density = 20 mA cm⁻², Na₂SO₄ concentration = 25 g L⁻¹, initial CIP
 78 concentration = 30 mg L⁻¹, and initial pH = 5).



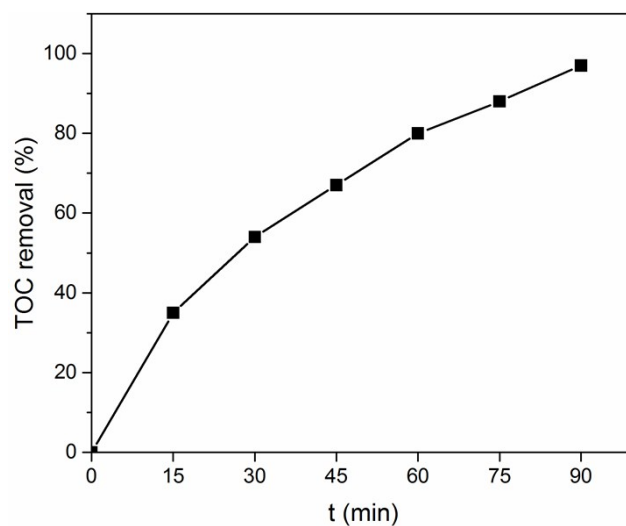
79

80 **Fig. S4** CV curves of the SSO-16 electrode with the absence and presence of CIP.



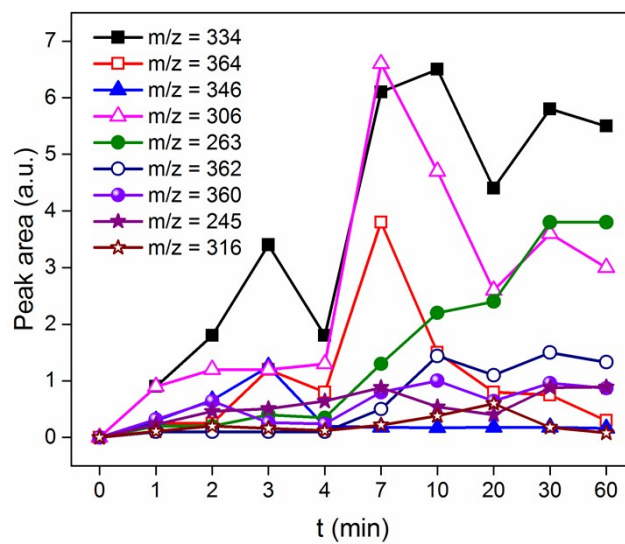
81

82 **Fig. S5** Fluorescence spectral of electrochemical oxidation of 0.5 mM terephthalic acid solution
83 with the SSO-16 electrode.



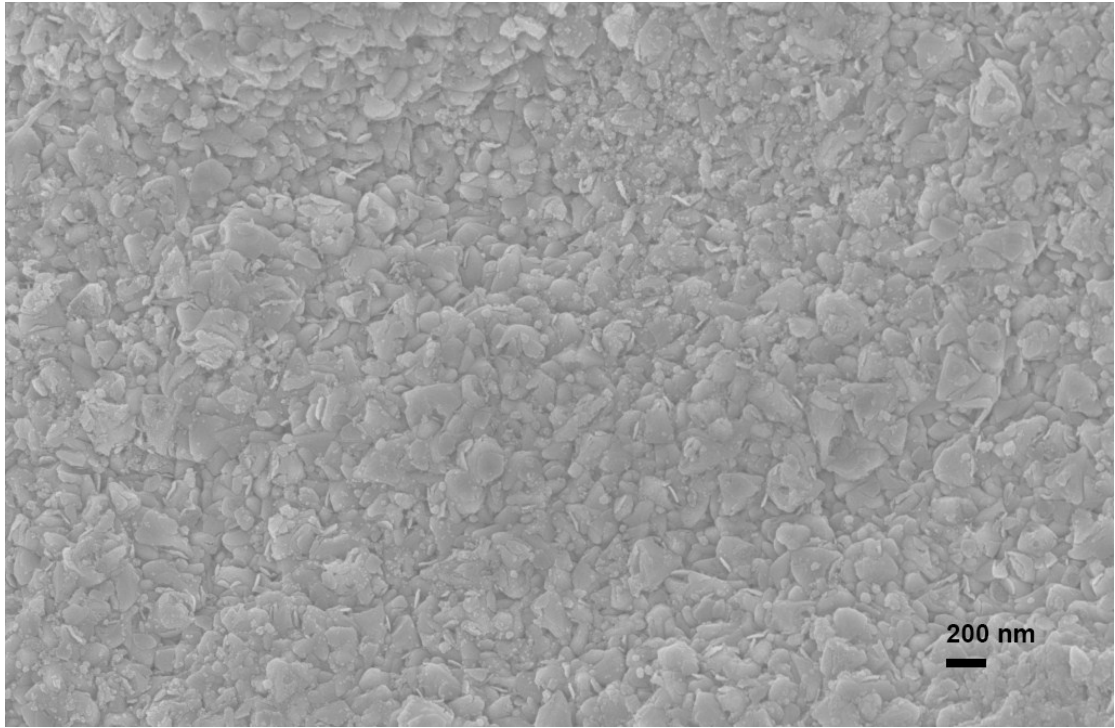
84

85 **Fig. S6** TOC removal ratio as a function of time under the optimal degradation conditions
86 (Current density = 20 mA cm⁻², Na₂SO₄ concentration = 25 g L⁻¹, initial CIP concentration = 30
87 mg L⁻¹, and initial pH = 5).



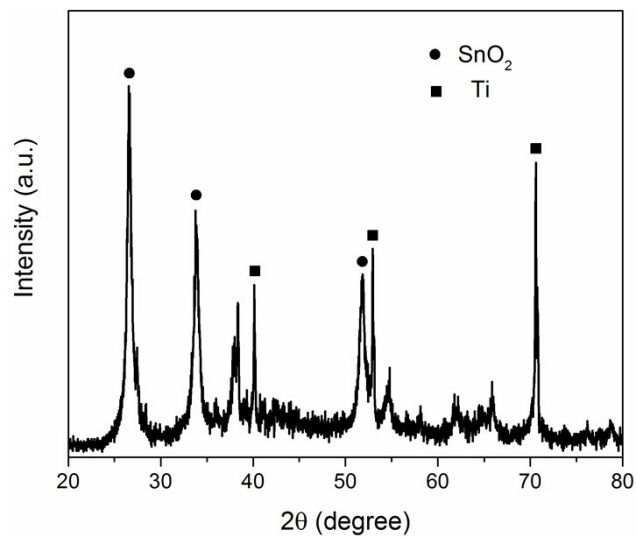
88

89 Fig. S7 Relative intensity variations of intermediates during the process of CIP degradation.



90

91 **Fig. S8** SEM image of the SSO-16 electrode after eight cycles of experiment.



92

93

Fig. S9 The XRD pattern of the SSO-16 electrode after eight cycles of experiment.